Multipeptide-Metalloporphyrin Assembly on a Dendrimer Template and Photoinduced Electron Transfer Based on the Dendrimer Structure

Muneyoshi Sakamoto,[a] Akihiko Ueno,[a] and Hisakazu Mihara*[a, b]

Abstract: To construct an artificial photosynthetic system, peptide dendrimers [*n*-(X-HLY)PAMAMs: X = R, E; Y = L, F; *n* = 4, 8, 16, 32 and 64 segments], in which amphiphilic α-helix peptides (X-HLY: R-HLL, E-HLL and R-HLF) were introduced at the end groups of polyamidoamine dendrimers (PAMAMs), were designed and synthesized. The peptide dendrimers 64-(X-HLY)-PAMAMs are novel synthetic biopolymers with an enormous molecular weight, about 160 kDa, and with a regulated amino acid sequence and three-dimensional conformation. The peptide dendrimers bound Fe^{III}- or Zn^{II}-mesoporphyrin IX per two α-helices; this afforded a multimetalloporphyrin assembly similar to the natural light-harvesting antennae in photosynthetic bacteria. Circular dichroism studies and peroxidase activity measurements revealed that metalloporphyrins were coordinated to the peptide dendrimers in a regulated manner and packed more densely with the growth of the dendrimer generation. Fluorescence quenching and photoreduction studies with methylviologen demonstrated that the photoinduced electron-transfer function with the peptide dendrimer-multi-Zn-MP was accomplished more effectively as the dendrimer generation increased. Thus, the three-dimensional assembly of metalloporphyrins and peptides in the dendrimer was an effective module for light-harvesting antennae in an artificial photosynthetic system.

Keywords: dendrimers · electron transfer · peptides · photochemistry · porphyrinoids

Introduction

Photoinduced electron transfer performs one of the most essential and important processes in photosynthesis. Therefore, it has been extensively studied for construction of an artificial photosynthetic system that uses electron transfer as an alternative energy resource to the dwindling fossil fuels.[1] In natural systems, the efficient electron-transfer function is due to supramolecular systems that consist of assemblies of peptides and functional groups. For instance, the light-harvesting antennae (LH) of photosynthetic bacteria,[2] in which many bacteriochlorophylls are assembled and oriented with α-helix peptides, absorb light energy, migrate, and transfer the energy to the reaction center where charge separation occurs.

[a] Prof. H. Mihara, M. Sakamoto, A. Ueno
Department of Bioengineering
Graduate School of Bioscience and Biotechnology
Tokyo Institute of Technology
Nagatsuta, Yokohama 226-8501 (Japan)
Fax: (+81) 45-924-5833
E-mail: hmihara@bio.titech.ac.jp

[b] Prof. H. Mihara
Form and Function, PRESTO
Japan Science and Technology Corporation
Tokyo Institute of Technology
Nagatsuta, Yokohama 226-8501 (Japan)

Numerous attempts have been made to develop such an artificial supramolecular photosynthetic system, which has more native-like properties and can remove the complexity of the natural counterparts, by the construction of de novo designed peptides[3, 4] and porphyrin-conjugated polymers.[5]

On the other hand, dendrimers have attracted much attention in the field of polymer chemistry.[6–12] Dendrimers are hyperbranched, artificial macromolecules with well-defined three-dimensional shapes, and their end groups are packed more densely as the number of their branch units increases. Unlike most synthetic macromolecules of linear chains, dendrimers directly adopt constructs of a higher-ordered structure. Therefore, their unique structures and functions have been exploited for molecular catalysts[8] and functional materials.[9] Particular attention has been focused on the possiblity of creating artificial photosynthesis modules from some dendrimers, due to their morphological similarity to LH.[10]

By using dendrimers as a template to combine de novo designed protein technologies, the assembly condition of the peptides and the functionalization may be controlled directly and exactly. In a previous study,[11] we developed peptide dendrimers that bound one Zn^{II}-mesoporphyrin IX (Zn-MP) per 2α-helix peptides equivalently, so that they formed multi-Zn-MP arrays. From the results of fluorescence studies with an anionic electron acceptor, naphthalene sulfonate (NS^-),[10b]

  0947-6539/01/0711-2449 $ 17.50+.50/0

and a cationic one, methylviologen (MV^{2+}),[10b, 13] it could be seen that the electron transfer properties were expressed more effectively with the growth of the dendrimer generations. By using MV^{2+}, the electron was transferred from multi-Zn-MP into the peptide dendrimers by dynamic interactions.[11]

In this study, to further examine the electron-transfer functions of the peptide dendrimer-multimetalloporphyrin conjugates, three amphiphilic α-helical peptides (X-HLY: R-HLL, E-HLL and R-HLF) were designed and introduced at the end groups (4, 8, 16, 32, and 64 segments) of polyamidoamine dendrimers (PAMAMs)[6] (Figure 1 and Figure 2, below). The Fe^{III}- or Zn^{II}-mesoporphyrins IX (Fe-MP or Zn-MP) were each coordinated between 2α-helix peptides[4, 11] to give a multimetalloporphyrin array (Figure 1a), which should pack more densely with the growth of the dendrimer generation. The electron transfer and the photoreduction of MV^{2+} were also accomplished more effectively as the dendrimer generation increased. Additionally, their reactivities, which depend on the amino acid sequence, such as on the hydrophobicity of the porphyrin binding site, and on the electrostatic field of the peptide-dendrimer outer shell, were evaluated.

Results and Discussion

Design and synthesis of peptide dendrimers: Synthesis of the peptide dendrimers was performed by using a domain-ligation strategy[12] by which the peptide and the template were prepared separately and then both parts were conjugated by ligation. The 20-residue peptides (X-HLY: R-HLL, E-HLL and R-HLF) were designed to take on an amphiphilic α-helical structure, which should be stabilized by four sets of Glu-Lys salt bridges (Figure 1b). X (Arg or Glu) was introduced at the C terminus of the peptides to form an electrostatic field through the positive guanidinium side chain of Arg or the negative carboxylate side chain of Glu at the outer shell of the peptide dendrimers. As an axial ligand of metalloporphyrin, His was introduced at the tenth position of the peptide to deploy a porphyrin parallel to the helix axis. Four hydrophobic residues [2 Leu and 2 Y (= 2 Leu or 2 Phe)] per α helix were arranged to construct a hydrophobic pocket surrounding the His residues as a porphyrin binding site (Figure 1c).[4, 11] The two 2 Y (2 Leu or 2 Phe) were employed to examine the influences of the hydrophobic residues on the metalloporphyrin coordination and on the electron-transfer properties through the porphyrin binding. Cys was used at the N terminus of the peptide to ligate to the outer termini of the template dendrimer through the thioether linkage. The peptides, X-HLY, were synthesized by the solid-phase method by using the Fmoc-strategy[14] and purified with reversed-phase HPLC (RP-HPLC). The purified peptides were identified by matrix-assisted laser-desorption ionization time-of-flight mass spectrometry (MALDI-TOFMS) and amino acid analysis.

PAMAM dendrimers[6] [outer terminal number (generation); $n = 4$ (G0), 8 (G1), 16 (G2), 32 (G3), and 64 (G4)] were selected as the dendrimer parts, since these were easy to handle and their amidoamine fragments resembled polypeptides. To conjugate the peptide with PAMAM, a chloroacetyl group was introduced at each amino terminal group of the PAMAM, by treating the peptide with *N*-ethyloxycarbonyl-2-ethyloxy-1,2-dihydroquinoline (EEDQ)[15] and chloroacetic acid in methanol. Perchloroacetylated PAMAMs (*n*-ClAc-PAMAMs) were purified by size-exclusion chromatography (SEC, Sephadex LH-60/MeOH) and RP-HPLC, and identified by MALDI-TOFMS. Then, X-HLY and *n*-ClAc-PAMAMs were combined by the ligation reaction[16] between the thiol side chain of Cys in X-HLY and the chloroacetyl group of *n*-ClAc-PAMAM. The peptide dendrimers, *n*-(X-HLY)PAMAMs (Figure 2), were purified by SEC (Sephadex G-50/30% AcOH) and RP-HPLC, and

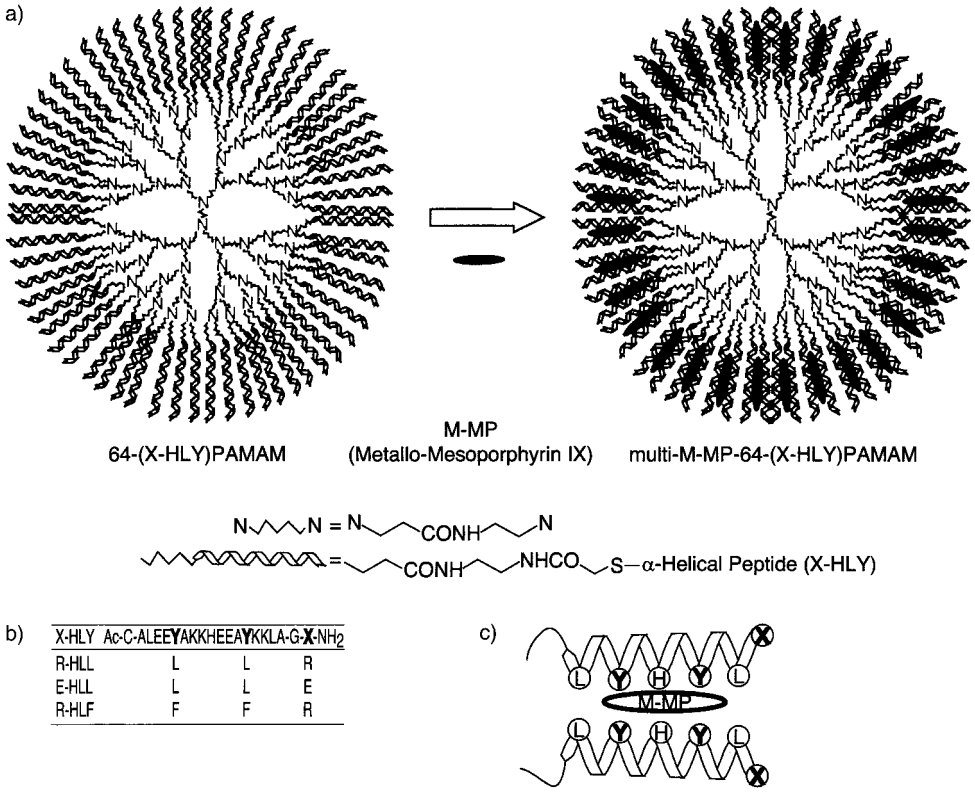

Figure 1. Structure of the peptide dendrimers: a) 64-(X-HLY)PAMAM and multi-M-MP-64-(X-HLY)PAMAM. b) Amino acid sequences of X-HLY (R-HLL, E-HLL and R-HLF). c) Schematic illustration of metalloporphyrin (M-MP) coordination to the 2α-helix of the peptide dendrimer.

0947-6539/01/0711-2450 $ 17.50+.50/0 *Chem. Eur. J.* **2001**, *7*, No. 11

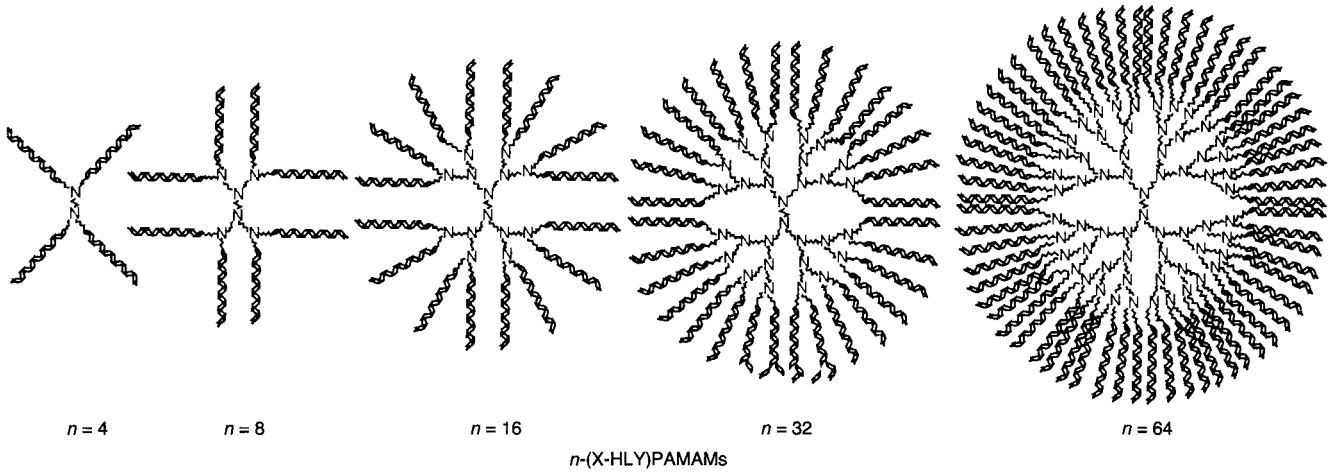

Figure 2. Illustration of the peptide dendrimers, *n*-(X-HLY)PAMAMs.

identified by MALDI-TOFMS ($n = 4$, 8) or ultracentrifugation ($n > 8$) (Table 1). The sedimentation equilibrium experiments revealed that these dendrimers were dispersed in a single species with a monomeric molecular weight. The 64-(X-HLY)PAMAM peptide dendrimers are novel synthetic biopolymers with an enormous molecular weight of about 160 kDa and a regulated amino acid sequence and three-dimensional structure.

Circular dichroism studies: Circular dichroism (CD) studies revealed that *n*-(X-HLY)PAMAMs ($n = 4$, 8, 16, 32, and 64), and those in the presence of Fe-MP showed a typical α-helical pattern in a buffer (Figure 3). Table 2 shows the α-helicity of the peptides in dendrimers estimated from the ellipticities (θ) at 222 nm.[17] The peptide dendrimers, *n*-(X-HLL)PAMAMs (X = R, E), with the different generations have similar α-helical properties (helix content, ca. 50 %) and the addition of Fe-MP did not alter the α-helix structure (Figure 3a, b). On the other hand, the α-helicities of *n*-(R-HLF)PAMAMs were lower than those of *n*-(X-HLL)PAMAMs (Figure 3c, dashed line). By addition of Fe-MP to *n*-(R-HLF)PAMAMs, the α-helicities were increased to 40–50 % (Figure 3c, solid line). These results indicated that the addition of Fe-MP to *n*-(R-HLF)PAMAMs stabilized their α-helix structure through the Fe-MP binding,[4a] and that the dendrimer structure afforded a similar α helicity so as to produce α-helical peptide dendrimers with the metalloporphyrins.

The Zn-MP coordinated to the peptide dendrimers showed strong induced CD peaks in the Soret region (Figure 4). In the

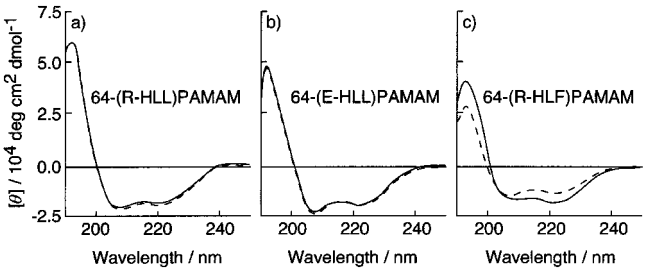

Figure 3. CD spectra in the amide region of 64-(X-HLY)PAMAMs: X-HLY = a) R-HLL, b) E-HLL, c) R-HLF; alone (dashed line) and in the presence of Fe-MP (solid line) in 20 mM Tris HCl buffer, pH 7.4 at 25 °C. [64-(X-HLY)PAMAM] = 10 μM (2α-helix conc.), [Fe-MP] = 10 μM.

presence of the lower-generation peptide dendrimers, 4-(X-HLY)PAMAMs, the Soret regions of Zn-MP were split into a negative peak at a longer wavelength and a positive peak at a shorter wavelength (Figure 4a). The crossover wavelengths were coincident with those of the Soret absorption maxima, and the intensities of the positive and negative peaks were almost equal; this indicated that the induced Soret CDs were derived from exciton coupling with (Zn-MP)–(Zn-MP) interactions. From the split Cotton effect, that is exciton coupling, Zn-MP-4-(X-HLY)PAMAM conjugates were assumed to form a four-helix bundle structure.[3] In the presence of the middle generation dendrimers, 8- or 16-(X-HLY)PAMAMs, negative CD peaks were diminished to give CD spectra with a symmetrical shape (Figure 4b, c). These facts suggested that the Zn-MP molecules in these peptide dendrimers were in a pseudospherical environment due to the dendrimer architecture, which affords a more spherical structure with increased dendrimer generation. In the presence of the higher-generation peptide dendrimers, 32- or 64-(X-HLY)-PAMAMs, negative CD peaks were generated again (Fig-

Table 1. Characterization of the peptide dendrimers.[a]

n-(X-HLY) PAMAM	R-HLL Found	R-HLL Calcd	E-HLL Found	E-HLL Calcd	R-HLF Found	R-HLF Calcd
Peptide alone	2281.6	2279.7	2254.1	2252.6	2349.0	2347.7
$n = 4$	9791.6	9792.9	9684.0	9683.2	10055.5	10063.6
$n = 8$	19900.9	19895.6	19770.0	19763.1	20552.9	20523.8
$n = 16$	37500 ± 2300	40356	44600 ± 2900	39922	47900 ± 8200	41444
$n = 32$	84800 ± 7700	81108	98900 ± 3700	80242	82500 ± 7600	83285
$n = 64$	155100 ± 5700	162612	173400 ± 6000	160880	149000 ± 4200	166966

[a] The peptides and the peptide dendrimers of lower generations ($n = 4$, $n = 8$) were identified by MALDI-TOFMS. The peptide dendrimers of higher generations ($n > 8$) were characterized by ultracentrifugation, since they were difficult to detect by MALDI-TOFMS.

Table 2. Molar ellipticities [θ] at 222 nm and α-helix contents of the peptide dendrimers and those in the presence of Fe-MP.

	Molar ellipticity $[\theta]_{222}$ [deg cm^2 d mol^{-1}] (α-helix content [%])[a]					
n-(X-HLY) PAMAM	R-HLL		E-HLL		R-HLF	
	Peptide alone	with Fe-MP	Peptide alone	with Fe-MP	Peptide alone	with Fe-MP
$n=4$	−16800 (53)	−16000 (51)	−14300 (45)	−15700 (50)	−8100 (26)	−12500 (39)
$n=8$	−16700 (53)	−16000 (51)	−16000 (51)	−15900 (50)	−10000 (32)	−12700 (40)
$n=16$	−15100 (48)	−14700 (47)	−15600 (49)	−16300 (51)	−10600 (34)	−12800 (39)
$n=32$	−14500 (46)	−14100 (45)	−15200 (48)	−16000 (51)	−10100 (32)	−13400 (42)
$n=64$	−14500 (46)	−14000 (45)	−15600 (49)	−16300 (51)	−12300 (39)	−16600 (52)

[a] Molar ellipticities and α-helix contents were estimated from CD spectra; [*n*-(X-HLY)PAMAM] = 10 μM (per 2α-helix conc.), [Fe-MP] = 10 μM.

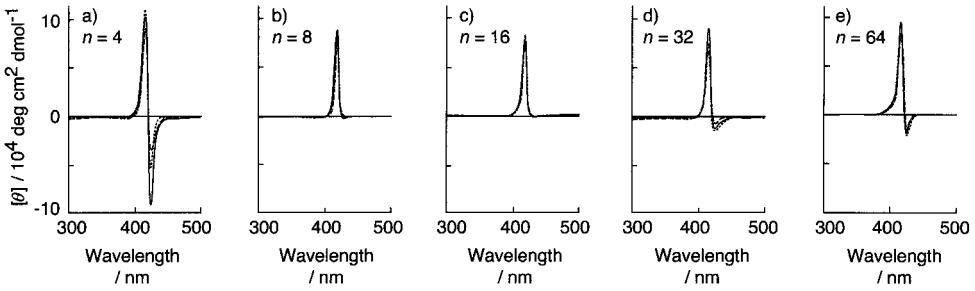

Figure 4. CD spectra in the Soret region of Zn-MP in the presence of *n*-(X-HLY)PAMAMs: a) $n=4$, b) $n=8$, c) $n=16$, d) $n=32$, e) $n=64$; R-HLL (solid line), E-HLL (dotted line), R-HLF (hatched line) in 20 mM Tris HCl buffer, pH 7.4 at 25 °C. [Zn-MP] = 5.0 μM, [*n*-(X-HLY)PAMAM] = 7.0 μM (2α-helix conc.).

ure 4d, e). It was assumed that, when the peptides and Zn-MPs were assembled more densely in the spherical architecture of the peptide dendrimers in higher generations, then the exciton coupling with (Zn-MP)–(Zn-MP) interactions was partially generated again. The differences in the CD shapes indicated that the orientation of Zn-MPs differed between the generations. The dendrimers with Fe-MP showed similar results to those with Zn-MP (data not shown). These results also suggested that Zn/Fe-MPs were coordinated to the peptide dendrimers in a regulated manner according to the dendrimer structure, and packed more densely with the growth of the dendrimer generation, as suggested by the peroxidase activity measurements (described below).

UV/Vis titration of metalloporphyrins (Fe-MP binding): To characterize Fe-MP binding with the peptide dendrimers, UV/Vis titration of Fe-MP with *n*-(X-HLY)PAMAMs was carried out in a buffer.[4] With increasing peptide concentration, an increase in the Soret band at 404 nm and a decrease in the band at 370 nm of Fe-MP were observed (Figure 5a). The binding constant (K_a) was determined from the absorbance change at 404 nm by using a single-site binding equation and assuming 1:1 (2 α-helices in the peptide dendrimer/Fe-MP) complexation (Figure 5a, inset).[18] Data for all the peptide dendrimers were fitted to this single-site binding equation; this indicated that the peptide dendrimer bound one Fe-MP per two α-helices and that the multi-Fe-MP array was achieved. The K_a values indicated that Fe-MP bound to the peptide dendrimers efficiently and that the binding affinities were almost identical at about $1-2\times10^6$ M^{-1} in the different generations of *n*-(X-HLL)PAMAMs (X = R, E) (Table 3). In the series of *n*-(R-HLF)PAMAMs, the binding affinities of Fe-MP were slightly larger than those of *n*-(X-HLL)PAMAMs. These results suggested that the introduction of a Phe

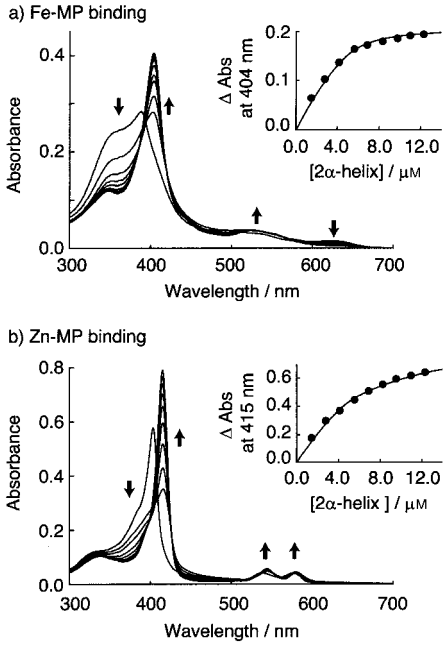

Figure 5. UV/Vis spectra of M-MP with increasing concentration of 64-(R-HLL)PAMAM in 20 mM Tris HCl buffer, pH 7.4 at 25 °C. [M-MP] = 5.0 μM. Insets: Plots of the absorbance change at the Soret absorbance maximum of M-MP as a function of 64-(R-HLL)PAMAM. a) M = Fe, absorption maximum = 404 nm. b) M = Zn, absorption maximum = 415 nm.

residue instead of Leu at the hydrophobic binding site of Fe-MP enhanced the Fe-MP binding, probably through *CH*-π interactions between the phenyl group of Phe and the pyrrole group of porphyrin.[4a]

(Zn-MP binding): To examine the photoinduced electron transfer properties, Zn^{II}-porphyrin was selected[1, 10, 11] and UV/Vis titration of Zn-MP with *n*-(X-HLY)PAMAMs was carried out

0947-6539/01/0711-2452 $ 17.50+.50/0 *Chem. Eur. J.* **2001**, *7*, No. 11

Table 3. Binding constants K_a for the peptide dendrimers with Fe-MP and Zn-MP.

n-(X-HLY)PAMAM	K_a[a] [10^5 M^{-1}]					
	R-HLL		E-HLL		R-HLF	
	Fe-MP	Zn-MP	Fe-MP	Zn-MP	Fe-MP	Zn-MP
$n=4$	13	3.1	12	4.0	19	6.8
$n=8$	14	3.5	16	3.9	29	8.6
$n=16$	18	4.9	17	3.5	37	7.7
$n=32$	20	5.3	21	3.5	37	9.4
$n=64$	21	5.3	20	3.4	39	9.8

[a] The binding constants K_a were estimated by UV/Vis spectra titration by using an single-site binding equation and assuming one metalloporphyrin to 2α-helices in the peptide dendrimer, in 20 mM Tris HCl buffer, pH 7.4 at 25 °C. [Fe-MP] = [Zn-MP] = 5.0 μM.

by the same method as described for Fe-MP binding. On addition of the peptide dendrimers, an increase in the Soret band at 415 nm and a decrease in the band at 403 nm of Zn-MP were observed (Figure 5b). The binding constant (K_a) was determined from the absorbance change at 415 nm by using a single-site binding equation and assuming a 1:1 (2 α-helices in the peptide dendrimer/Zn-MP) complexation (Figure 5b, inset). All the peptide dendrimers bound one Zn-MP for each two α-helices and formed multi-Zn-MP arrays. The K_a values indicated that Zn-MP bound to the peptide dendrimers effectively and that the binding affinities to the peptide dendrimers were almost identical at about $3-5\times10^5$ M^{-1} in the different generations of *n*-(X-HLL)PAMAMs (X = R, E) (Table 3). In the series of *n*-(R-HLF)PAMAMs, the binding affinities of Zn-MP were also higher than those of *n*-(X-HLL)-PAMAMs. These results for Zn-MP coincided with those for Fe-MP. The affinities of Fe-MP were higher than those of Zn-MP, probably due to the difference between coordination states of Fe-MP and Zn-MP to the peptide dendrimers. It is possible that the stable states are 6-coordinated and 5-coordinated for the Fe− and Zn-MP, respectively.[4a]

Peroxidase-like activities: In order to examine the catalytic activity of Fe-MP as regulated by the binding of the peptide dendrimers, peroxidase-like activity was demonstrated by following the oxidation reaction of 2-methoxyphenol to its tetramer, tetraguaiacol (Scheme 1).[4a,b] This reaction is one of the typical reactions catalyzed by peroxidase or mono-oxygenase in the family of hemenzymes. In the design of Fe-MP conjugated peptides, Fe-MP was fixed in the polypeptide three-dimensional structure by the bis-His coordination,

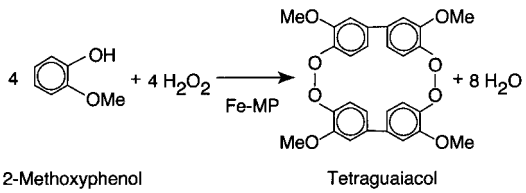

Scheme 1. The oxidation of 2-methoxyphenol in the presence of Fe-MP.

similar to natural *b*-type hemeproteins. Thus, as the peptide binds Fe-MP more tightly, Fe-MP reacts less readily with a substrate, such as hydrogen peroxide.[4a,b] The reaction was initiated by the addition of hydrogen peroxide (0.5 mM) to a solution containing 2-methoxyphenol (10 mM), multi-Fe-MP-*n*-(X-HLY)PAMAMs (5.0 μM of Fe-MP, 7.0 μM of the peptide dendrimers per 2α-helix). In this condition, 80–90 % (4.0–4.5 μM) of Fe-MP was coordinated to the peptide dendrimer. The determined initial rates (v_0) are summarized in Figure 6.

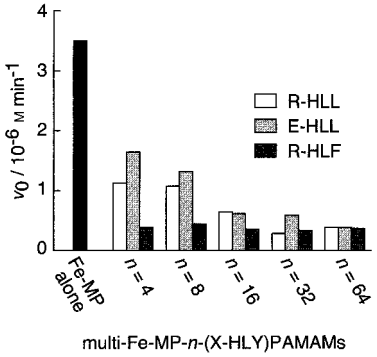

Figure 6. Initial rates (v_0) of tetraguaiacol formation catalyzed by Fe-MP (Fe-MP alone, black) in the presence of *n*-(R-HLL)PAMAMs (white), *n*-(E-HLL)PAMAMs (light gray) and *n*-(R-HLF)PAMAMs (dark gray) in 0.1 M Tris HCl buffer, pH 7.4 at 25 °C. [Fe-MP] = 5.0 μM, [*n*-(X-HLY)PAMAM] = 7.0 μM (2α-helix conc.), [2-methoxyphenol] = 10 mM, [H_2O_2] = 0.5 mM.

The initial rates of the reactions in the presence of the peptide dendrimers were suppressed more with the growth of the dendrimer generation. This result implied that Fe-MPs bound more tightly when the packing was denser, that is, in the higher dendrimer generations. Especially, the initial rates of the reactions in multi-Fe-MP-*n*-(R-HLF)PAMAMs were suppressed even at $n=4$; this indicated that Fe-MP was coordinated much more tightly by using Phe at the binding site.

Fluorescence studies: To examine the photoinduced electron transfer properties of multi-Zn-MP-*n*-(X-HLY)PAMAMs, fluorescence quenching studies were performed by the addition of methylviologen (MV^{2+}).[10b, 11, 13] Upon excitation at the Q-band (545 nm), multi-Zn-MP-*n*-(X-HLY)PAMAMs emitted fluorescence bands at 584 and 630 nm that were quenched by the addition of MV^{2+} (Figure 7a). Stern–Volmer plots showed that the fluorescence quenching occurred more strongly with the growth of the generation (Figure 7b). Table 4 summarizes the Stern–Volmer constants (K_{SV}) for the fluorescence quenching study, calculated from the Stern–Volmer equation.[19] In each generation, the relative concentrations of the 2α-helix and Zn-MP were constant (the solution contained 5.0 μM of Zn-MP and 7.0 μM of *n*-(R-HLL)PAMAM per 2α-helix), in which 65 % of Zn-MP (3.2 μM) was coordinated to the peptide dendrimers. Consequently, the electron-transfer property was amplified by the designed dendrimer structure.

In the comparison of the positively charged multi-Zn-MP-64-(R-HLY)PAMAMs (Y = L, F), the Stern–Volmer plots were linear, and the fluorescence quenching with multi-Zn-MP-64-(R-HLF)PAMAM was more effectively expressed (1.3 times) than with multi-Zn-MP-64-(R-HLL)PAMAM. Since the Phe-containing dendrimers bound Zn-MP more

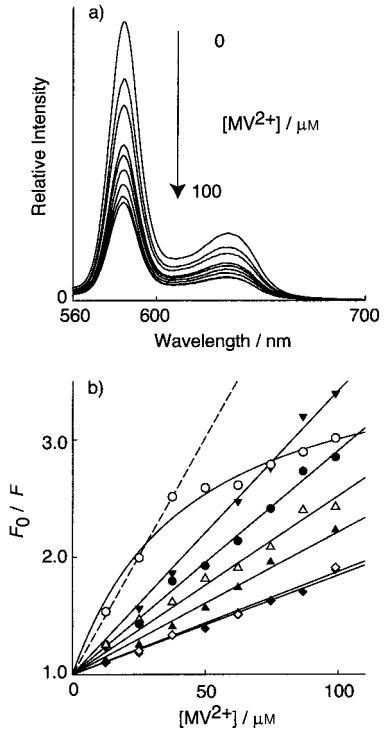

Figure 7. a) Fluorescence spectra of multi-Zn-MP-64-(R-HLL)PAMAM with the addition of MV^{2+} in 20 mM Tris buffer, pH 7.4 at 25 °C. λ_{ex} = 545 nm. [Zn-MP] = 5.0 μM, [64-(R-HLL)PAMAM] = 7.0 μM (2α-helix conc.), [MV^{2+}] = 0 – 100 μM. b) The Stern – Volmer plots for fluorescence quenching of multi-Zn-MP-*n*-(R-HLL)PAMAMs: n = 4 (◆), n = 8 (◇), n = 16 (▲), n = 32 (△), n = 64 (●), and those of 64-(X-HLY)PAMAMs: E-HLL (○), R-HLF (▼) by the addition of MV^{2+} in 20 mM Tris buffer, pH 7.4 at 25 °C. λ_{ex} = 545 nm, λ_{em} = 584 nm. [Zn-MP] = 5.0 μM, [*n*-(X-HLY)PAMAM] = 7.0 μM (2α-helix conc.), [MV^{2+}] = 0 – 100 μM.

strongly than the Leu-containing dendrimers (Table 3), the effective Zn-MP binding to α-helix peptides affected the efficient electron transfer within the same generation of the dendrimers. The Stern – Volmer plot for the negatively charged multi-Zn-MP-64-(E-HLL)PAMAM and MV^{2+} system showed a highly efficient fluorescence quenching even at a lower concentration of MV^{2+}. In contrast, for higher concentrations of MV^{2+}, the fluorescence quenching was clearly saturated. Considering the result, this saturation behavior indicates the binding of MV^{2+} molecules to the negatively charged surface of the peptide dendrimer by electrostatic forces.[10b]

To confirm the electrostatic interaction in the ground state, UV/Vis spectra were measured when MV^{2+} had been added.[11] In the case of the negatively charged multi-Zn-MP-64-(E-HLL)PAMAM, the Q-band decreased (by ca. 20 %) evidently due to the addition of MV^{2+}; this supported the idea of electrostatic binding between multi-Zn-MP-64-(E-HLL)PAMAM and MV^{2+} in the ground state. By contrast, in the case of the positively charged multi-Zn-MP-64-(R-HLY)-PAMAMs (Y = L, F), UV/Vis spectra were little changed by the addition of MV^{2+}; this indicated that MV^{2+} does not have a strong influence in the ground state of Zn-MP. Consequently, the electron-transfer mechanisms were different between the positively charged peptide dendrimer-multi-Zn-MP and the negatively charged one. That is, electron transfer based on dynamic interactions occurred in the cationic peptide dendrimer-multi-Zn-MP and MV^{2+} system, while electron transfer through electrostatic binding took place in the anionic one.[11]

To examine the reason for the fluorescence quenching magnification through the dendrimer architecture, the fluorescence lifetime of Zn-MP conjugated with the peptide dendrimers was measured in the absence of the quencher MV^{2+}. Table 5 shows the fluorescence lifetime parameters of Zn-MP conjugated with the peptide dendrimers, in which the fluorescence decay profiles were analyzed by the double-exponential equation satisfactorily.[10b] Under these conditions, about 65 % of Zn-MP (3.2 μM) was bound to *n*-(R-HLL)PAMAMs, which corresponded to the percentage (A_1) of the short-lived species (τ_1). The fluorescence lifetime (τ_1) of Zn-MP coordinated to *n*-(R-HLL)PAMAMs decreased according to the generation increase of the dendrimers [1.8 ns (n = 4) to 1.2 ns (n = 64)]. With the growth of the dendrimer generation, Zn-MPs were packed more densely in the peptide dendrimer, so that the excitation energy might migrate among the neighboring Zn-MPs and the fluorescence lifetimes were shortened.[20] The rate constant (k_{ent}) for the energy transfer in the neighboring Zn-MPs and the yield of the energy transfer (Φ_{ent}) were estimated by using the equations[21] described in Table 5. At the highest generation, n = 64, k_{ent} was $3.6 \times 10^8\ s^{-1}$, which was faster than that of the lowest generation, n = 4, $0.8 \times 10^8\ s^{-1}$, this indicated that the excitation energy was delocalized in the neighboring Zn-MPs more effectively with the generation growth. Thus, the yields of the energy transfer (Φ_{ent}) were also enhanced by the generation growth. This delocalization of light energy by intercomplex energy transfer through the dendrimer architecture was assumed to induce the effective electron transfer in a similar way to natural LH.[2] In the case of 64-(R-HLF)PAMAM, 76 % of Zn-MP (3.8 μM) was bound; this corresponded to the fluorescence decay component (τ_1), and the lifetime was greatly shortened (0.7 ns, 76.8 %). The rate constant for the energy transfer ($k_{ent} = 9.5 \times 10^8\ s^{-1}$) was much faster than that for 64-(R-HLL)PAMAM. These results indicated that Zn-MP was bound strongly in the Phe-peptide dendrimer, so that the electron transfer to MV^{2+} was improved.

Table 4. The Stern – Volmer constants (K_{SV}) of fluorescence quenching by the addition of MV^{2+} and the parameters of photoreduction of the MV^+ radical.

Peptide dendrimer multi-Zn-MP	K_{SV}[a] [10^4 M^{-1}]	MV^{2+} Photoreduction parameters v_0[b] [10^{-6} M min^{-1}]	$[MV^+]_{10}$[c] [10^{-6} M]
Zn-MP alone	0.9	1.1	4.2
4-(R-HLL)PAMAM	0.9	1.6	5.1
8-(R-HLL)PAMAM	0.9	1.8	5.1
16-(R-HLL)PAMAM	1.2	2.2	5.8
32-(R-HLL)PAMAM	1.5	2.3	6.5
64-(R-HLL)PAMAM	1.9	2.6	8.0
64-(E-HLL)PAMAM	(4.0)[d]	2.4	6.7
64-(R-HLF)PAMAM	2.4	–[e]	–[e]

[a] The Stern – Volmer constants K_{SV} were calculated by the Stern – Volmer equation, $F_0/F = 1 + K_{SV}$ [MV^{2+}], from fluorescence quenching studies. [b] Initial rates for accumulation of the MV^+ radical. [c] Amount of the MV^+ radical after 10 min irradiation. [d] The constant was estimated in a lower concentration of MV^{2+} (Figure 7b, dashed line), since the Stern – Volmer plot with 64-(E-HLL)PAMAM was saturated at the higher concentration of MV^{2+}. [e] Data were not obtained due to the precipitation of 64-(R-HLF)PAMAM during the deaeration.

0947-6539/01/0711-2454 $ 17.50+.50/0 *Chem. Eur. J.* **2001**, *7*, No. 11

Table 5. Fluorescence lifetimes (τ) and molar fractions (A) for the peptide dendrimers-multi-Zn-MP and the calculated parameters of inter complex energy transfer.

Peptide dendrimer-multi-Zn-MP	Lifetime[a] τ_1 [ns]	A_1 [%]	τ_2 [ns]	A_2 [%]	χ^2	k_{ent}[b] [10^8 s^{-1}]	Φ_{ent}[c]
Zn-MP alone	–	–	2.1	100.0	1.17	–	–
4-(R-HLL)PAMAM	1.8	63.5	2.1	36.5	0.87	0.8	0.14
8-(R-HLL)PAMAM	1.8	64.3	2.0	35.7	1.15	0.8	0.14
16-(R-HLL)PAMAM	1.5	64.6	2.3	35.4	1.15	1.9	0.29
32-(R-HLL)PAMAM	1.4	62.4	2.0	37.6	1.20	2.4	0.33
64-(R-HLL)PAMAM	1.2	67.2	2.1	32.8	1.13	3.6	0.43
64-(E-HLL)PAMAM	1.3	60.2	2.1	39.8	1.20	2.9	0.38
64-(R-HLF)PAMAM	0.7	76.8	1.9	23.2	1.02	9.5	0.67

[a] Fluorescence lifetimes were measured by using Zn-MP (5.0 μM) conjugated with *n*-(X-HLY)PAMAMs (7.0 μM per 2α-helix conc.) in 20 mM Tris HCl buffer pH 7.4 at 25 °C. $\lambda_{ex} = 545$ nm, $\lambda_{em} > 570$ nm. Decay profiles were analyzed by the double exponential equation, $I_f(t) = A_1\exp(-t/\tau_1) + A_2\exp(-t/\tau_2)$. [b] The rate constants (k_{ent}) of energy transfer were calculated with the equation, $k_{ent} = 1/\tau_1 - 1/\tau_0$, in which τ_0 is the lifetime of the reference compound, Zn-MP alone (2.1 ns). [c] The yield of the energy transfer (Φ_{ent}) was calculated with the equation:

Photoreduction of methylviologen: In order to know that the peptide dendrimer-multi-Zn-MP functions as a photosensitizer for the artificial photosynthesis process, accumulation of the reduced MV^+ radical was performed by the three-component photoreduction system shown in Scheme 2.[22]

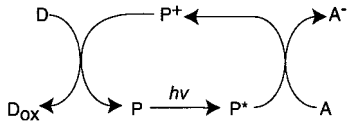

Scheme 2. The three-component photoreduction system: triethanolamine as an electron donor (D), the peptide dendrimer-multi-Zn-MP as a photosensitizer (P), and MV^{2+} as an electron acceptor (A).

When a solution containing triethanolamine, multi-Zn-MP-*n*-(X-HLL)PAMAMs ($n = 4$, 8, 16, 32, 64; X = R, E) and MV^{2+} was deaerated and irradiated, the solution turned blue immediately; this indicated the production of MV^+ radicals (Figure 8). Figure 9 shows the time-dependent accumulation of MV^+ radicals, which was measured by the absorbance at 602 nm (MV^+ radical, $\varepsilon = 1.37 \times 10^4$ M^{-1} cm^{-1}). In the case of multi-Zn-MP-*n*-(R-HLL)PAMAMs, the photoreduction of MV^{2+} was expressed more effectively with the increase in the dendrimer generation (Figure 9a). This result implied that the three-dimensional assembly of metalloporphyrin with the peptide dendrimer functioned as an effective photosensitizer in the artificial photosynthetic system. Table 4 summarizes the parameters for the production of MV^+ radicals and the Stern–Volmer constants (K_{SV}) from the fluorescence quenching study. In the multi-Zn-MP-*n*-(R-HLL)PAMAMs, the photoreduction parameters were comparable to the K_{SV} values; this indicated that the electron transfer from the peptide dendrimer-multi-Zn-MP to MV^{2+} would be the rate-determining step in this system.[1] Unfortunately, the photoreduction of MV^{2+} by using multi-Zn-MP-*n*-(R-HLF)PAMAMs was difficult to estimate due to the formation of precipitates during the deaeration. In the comparison of the positively charged peptide dendrimer, multi-Zn-MP-64-(R-HLL)PAMAM, and the negatively charged one, multi-Zn-MP-64-(E-HLL)PAMAM, the photoreduction of MV^{2+} by using the positive dendrimer was more effectively expressed (1.2 times)

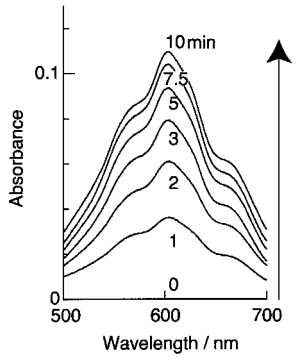

Figure 8. Absorption spectra of the MV^+ radical with multi-Zn-MP-64-(R-HLL)PAMAM, taken at 0, 1, 2, 3, 5, 7.5, and 10 min under steady state irradiation in 20 mM Tris HCl buffer, pH 7.4 at 25 °C. To remove complications, the absorbance of Zn-MP was subtracted. [triethanolamine] = 330 mM, [Zn-MP] = 5.0 μM, [64-(R-HLL)PAMAM] = 7.0 μM (2α-helix conc.), [MV^{2+}] = 50 μM.

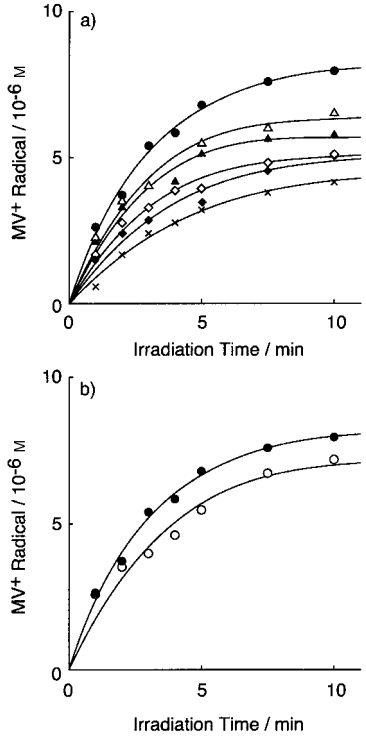

Figure 9. Time-dependent accumulation of the MV^+ radical under steady state irradiation: a) with multi-Zn-MP-*n*-(R-HLL)PAMAMs: $n = 4$ (◆), $n = 8$ (◇), $n = 16$ (▲), $n = 32$ (△), $n = 64$ (●), and Zn-MP alone (×). b) with multi-Zn-MP-64-(X-HLL)PAMAMs: X = R (●) and X = E (○) in 20 mM Tris HCl buffer, pH 7.4 at 25 °C. [triethanolamine] = 330 mM, [Zn-MP] = 5.0 μM, [*n*-(X-HLY)PAMAM] = 7.0 μM (2α-helix conc.), [MV^{2+}] = 50 μM.

than that with the negative one (Figure 9b). The difference was attributed to the influence of the electrostatic interaction in the ground state; that is, the positively charged multi-Zn-MP-64-(R-HLL)PAMAM does not bind MV^{2+} strongly in the ground state, while the negatively charged multi-Zn-MP-64-(E-HLL)PAMAM binds MV^{2+} by an electrostatic interaction. This interaction maintained the negative peptide dendrimer-multi−Zn-MP and MV^{2+} in close proximity, so that the back electron transfer from the reduced MV^{+} radical to the peptide dendrimer-multi-Zn-MP occurred more easily. These results indicate that electron transfer based on the relatively dynamic interaction between the cationic dendrimer and the cationic MV^{2+} is preferable for the effective accumulation of the reduced MV^{+} radical.

Conclusion

To construct an artificial photosynthetic system, peptide dendrimers, in which amphiphilic α-helix peptides were introduced at the end groups of polyamidoamine dendrimers, were successfully designed and synthesized. These peptide dendrimers are novel synthetic biopolymers with an enormous molecular weight, about 160 kDa, and with a regulated amino acid sequence and three-dimensional conformation like large-sized proteins. The peptide dendrimers bound metalloporphyrins per two α-helices; this formed the multi-metalloporphyrin array. Their electron transfer functions were accomplished more effectively with the growth of the dendrimer generation. This magnification of the electron transfer property was assigned to the fact that metalloporphyrins were packed more densely due to the dendrimer architecture, so that the light energy was delocalized across the neighboring metalloporphyrins, and then effective electron transfer occurred in a similar way to in the natural light-harvesting antennae in photosynthetic bacteria.[2] Additionally, by using MV^{2+} as an electron acceptor, the fluorescence quenching and the photoreduction with the positively charged peptide dendrimer were superior to those with the negatively charged one, in spite of the fact that the cationic peptide dendrimer did not strongly interact with the cationic MV^{2+} in the ground state. These results demonstrated that the three-dimensional assembly of Zn-MP with the peptide dendrimer was effective for a light-harvesting antennae in an artificial photosynthetic system, and that electron transfer, according to the dynamic interaction between the peptide dendrimer-multi-Zn-MP and viologen, was favorable for the function. This characteristic is also beneficial to a catalytic cycle. This approach is important in the development of an artificial photosynthesis and a novel photo devise. Moreover, photo-induced hydrogen evolution by using the peptide dendrimer-multi-Zn-MP-photosynthetic system and the enzyme, hydrogenase, was successfully demonstrated by the growth of the dendrimer generation.[23] Detailed studies are ongoing.

Experimental Section

Materials and methods: All chemicals and solvents were of reagent or HPLC grade. Mesoporphyrin IX was purchased from Aldrich and was converted to the Zinc and Ferric complexes by heating under reflux with excess $Fe(OAc)_2$ or $Zn(OAc)_2$ in acetic acid.[24] Amino acid derivatives and reagents for peptide synthesis were purchased from Watanabe Chemical Co. (Hiroshima, Japan). Polyamidoamine dendrimers [Starburst (PAMAM) Dendrimers: the number of outer terminal groups (generation); $n=4$ (G0), $n=8$ (G1), $n=16$ (G2), $n=32$ (G3) and $n=64$ (G4)] were purchased from Aldrich. MALDI-TOFMS was measured on a Shimadzu MALDI-III mass spectrometer by using 3,5-dimethoxy-4-hydroxycinnamic acid (Aldrich) as a matrix. Ultracentrifugation was performed with a Beckman Optima XL machine. Amino acid analyses were carried out by using phenylthiocarbamyl amino acids on RP-HPLC after hydrolysis of the peptides at 110 °C, for 24 h in a sealed tube.

Peptide synthesis: α-Helical peptides, X-HLY (R-HLL, E-HLL and R-HLF); Ac-Cys(Trt)-Ala-Leu-Glu(*t*Bu)-Glu(*t*Bu)-Y-Ala-Lys (Boc)-Lys-(Boc)-His(Trt)-Glu(*t*Bu)-Glu(*t*Bu)-Ala-Y-Lys(Boc)-Lys(Boc)-Leu-Ala-Gly-X-NH-Rink Resin [X = Arg(Mtr), Glu(*t*Bu); Y = Leu, Phe; Boc = *tert*-butoxy-carbonyl; Trt = trityl; Mtr = 4-methoxy-2,3,6-trimethyl-benzenesulfonyl] were synthesized by the Fmoc solid-phase method[14] by using Fmoc-protected amino acid derivatives (3.0 equiv), benzotriazole-1-yl-oxy-tris-(dimethylamino)phosphonium hexafluorophosphate (BOP, 3.0 equiv) and 1-hydroxybenzotriazole (HOBt, 3.0 equiv) on Rink amide resin (Advanced Chemtech.). The protecting groups and the resin were removed by stirring the dried resin with trifluoroacetic acid (TFA), *m*-cresol, ethanedithiol, thioanisole, and TMSBr for 1 h at 25 °C. Crude peptides were purified by RP-HPLC on YMC C4 Pack column (10 × 250 mm) by using a linear gradient of acetonitrile (ACN)/0.1 % TFA (1.0 % min^{-1}). The peptides were identified by MALDI-TOFMS and amino acid analysis. MALDI-TOFMS: R-HLL, 2281.6 $[MH]^+$ (calcd 2279.7); E-HLL, 2254.1 $[MH]^+$ (calcd 2252.6); R-HLF, 2349.0 $[MH]^+$ (calcd 2347.7); amino acid analysis, found (calcd): R-HLL $Ala_{4.00}$ (4), $Arg_{1.01}$ (1), $Glu_{3.69}$ (4), $Gly_{1.13}$ (1), $His_{1.17}$ (1), $Leu_{4.22}$ (4), $Lys_{3.76}$ (4); E-HLL $Ala_{4.00}$ (4), $Glu_{5.35}$ (5), $Gly_{1.04}$ (1), $His_{1.05}$ (1), $Leu_{4.11}$ (4), $Lys_{3.96}$ (4); R-HLF $Ala_{4.00}$ (4), $Arg_{1.05}$ (1), $Glu_{4.15}$ (4), $Gly_{1.24}$ (1), $His_{1.14}$ (1), $Leu_{2.14}$(2), $Lys_{4.05}$ (4), $Phe_{2.02}$ (2).

Synthesis of perchloroacetylated PAMAMs (*n*-ClAc-PAMAMs): A solution of PAMAM (number of outer terminal groups $n=4$, 8, 16, 32, and 64), *N*-ethyloxycarbonyl-2-ethyloxy-1,2-dihydroquinoline[15] (EEDQ, 5 equiv per amino group in PAMAMs), and chloroacetic acid (5 equiv) in methanol (1.0 mL) was stirred at room temperature under a nitrogen atmosphere for 1 – 7 days. To remove excess EEDQ and chloroacetic acid, the reaction mixture was treated by size-exclusion chromatography (SEC, Sephadex LH-60/MeOH, Pharmacia Biochemtech.). Then the products were purified by RP-HPLC (YMC, C4 Pack 10 × 250 mm) by using a linear gradient of ACN/0.1 % TFA (1.0 % min^{-1}) and identified by MALDI-TOFMS. *n*-ClAc-PAMAM: $n=4$, 823.6 $[MH]^+$ (calcd 823.6); $n=8$, 2065.7 $[MNa]^+$ (calcd 2064.7); $n=16$, 4483.0 $[MH]^+$ (calcd 4480.9); $n=32$, 9355.3 $[MH]^+$ (calcd 9357.4); $n=64$, 19130.6 $[MNa]^+$ (calcd 19133.7).

Synthesis of peptide dendrimers: A solution of the peptides (X-HLY: R-HLL, E-HLL and R-HLF) and corresponding *n*-ClAc-PAMAMs ($n=4$, 8, 16, 32, and 64; peptide: *n*-ClAc−PAMAM = 1.5*n*:1) in a 0.1 M Tris HCl buffer (pH 8.5) was stirred at room temperature for 48 h under a nitrogen atmosphere. To remove excess peptide, the reaction mixture was chromatographed by SEC (Sephadex G-50/30 % acetic acid), and then the products were purified by RP-HPLC (YMC, C4 Pack 10 × 250 mm) by using a linear gradient of ACN/0.1 % TFA (1.0 % min^{-1}) and identified by MALDI-TOFMS or ultracentrifugation (Table 1). Amino acid analysis, found (calcd): 4-(R-HLL)PAMAM $Ala_{16.0}$ (16), $Arg_{4.08}$ (4), $Glu_{16.1}$ (16), $Gly_{4.96}$ (4), $His_{4.32}$ (4), $Leu_{17.3}$ (16), $Lys_{15.6}$ (16); 8-(R-HLL)PAMAM $Ala_{32.0}$ (32), $Arg_{7.60}$ (8), $Glu_{32.2}$ (32), $Gly_{9.28}$ (8), $His_{8.08}$ (8), $Leu_{35.0}$ (32), $Lys_{29.2}$ (32); 16-(R-HLL)PAMAM $Ala_{64.0}$ (64), $Arg_{15.5}$ (16), $Glu_{62.7}$ (64), $Gly_{19.4}$ (16), $His_{16.8}$ (16), $Leu_{68.9}$ (64), $Lys_{63.8}$ (64); 32-(R-HLL)PAMAM $Ala_{128.0}$ (128), $Arg_{35.2}$ (32), $Glu_{118.7}$ (128), $Gly_{38.0}$ (32), $His_{35.2}$ (32), $Leu_{130.2}$ (128), $Lys_{121.3}$ (128); 64-(R-HLL)PAMAM $Ala_{256.0}$ (256), $Arg_{62.1}$ (64), $Glu_{247.0}$ (256), $Gly_{71.4}$ (64), $His_{69.8}$ (64), $Leu_{288.0}$ (256), $Lys_{248.3}$ (256); 4-(E-HLL)PAMAM $Ala_{16.0}$ (16), $Glu_{21.8}$ (20), $Gly_{5.60}$ (4), $His_{4.48}$ (4), $Leu_{16.7}$ (16), $Lys_{15.6}$ (16); 8-(E-HLL)PAMAM $Ala_{32.0}$ (32), $Glu_{45.5}$ (40), $Gly_{8.56}$ (8), $His_{8.80}$ (8), $Leu_{33.8}$ (32), $Lys_{31.7}$ (32); 16-(E-HLL)PAMAM $Ala_{72.0}$ (64), $Glu_{81.6}$ (80), $Gly_{17.7}$ (16), $His_{16.0}$ (16), $Leu_{70.4}$ (64), $Lys_{62.6}$ (64); 32-(E-HLL)PAMAM $Ala_{128.0}$ (128), $Glu_{176.0}$ (160), $Gly_{37.1}$ (32), $His_{34.6}$ (32), $Leu_{131.5}$ (128), $Lys_{128.3}$ (128); 64-(E-HLL)PAMAM $Ala_{256.0}$ (256), $Glu_{374.4}$ (320), $Gly_{64.3}$ (64), $His_{71.0}$ (64), $Leu_{282.9}$ (256), $Lys_{277.8}$ (256); 4-(R-HLF)PAMAM $Ala_{16.0}$ (16), $Arg_{5.08}$ (4), $Glu_{16.7}$ (16), $Gly_{5.72}$ (4), $His_{4.80}$ (4), $Leu_{10.0}$ (8), $Lys_{16.4}$ (16), $Phe_{10.2}$ (8); 8-(R-HLF)PAMAM $Ala_{32.0}$ (32), $Arg_{7.84}$ (8), $Glu_{35.6}$ (32), $Gly_{10.9}$ (8), $His_{8.16}$ (8),

0947-6539/01/0711-2456 $ 17.50+.50/0 *Chem. Eur. J.* **2001**, *7*, No. 11

$Leu_{16.0}$ (16), $Lys_{30.4}$ (32), $Phe_{19.4}$ (16); 16-(R-HLF)PAMAM $Ala_{64.0}$ (64), $Arg_{17.9}$ (16), $Glu_{69.1}$ (64), $Gly_{21.6}$ (16), $His_{17.9}$ (16), $Leu_{34.7}$ (32), $Lys_{65.4}$ (64), $Phe_{39.8}$ (32); 32-(R-HLF)PAMAM $Ala_{112.0}$ (128), $Arg_{35.8}$ (32), $Glu_{128.6}$ (128), $Gly_{49.9}$ (32), $His_{45.1}$ (32), $Leu_{58.9}$ (64), $Lys_{127.8}$ (128), $Phe_{64.0}$ (64); 64-(R-HLF)PAMAM $Ala_{256.0}$ (256), $Arg_{65.9}$ (64), $Glu_{279.7}$ (256), $Gly_{92.8}$ (64), $His_{76.8}$ (64), $Leu_{127.4}$ (128), $Lys_{243.2}$ (256), $Phe_{147.2}$ (128).

CD measurements: CD spectra were recorded on a Jasco J-720 spectropolarimeter by using a quartz cell with a 1.0 mm pathlength in the amide region (190–250 nm) and 10 mm in the Soret region (300–500 nm). The preparations of the samples were related as follows. *Amide region*: The peptide dendrimers were dissolved in 20 mM Tris HCl buffer, pH 7.4 at 25 °C. [*n*-(R-HLY)PAMAM] = 10 μM per 2α-helix. For the measurements in the presence of Fe-MP, Fe-MP (10 μM) and the peptide dendrimers (10 μM per 2α-helix) were dissolved in 20 mM Tris HCl buffer, pH 7.4, and the samples were equilibrated for 20 min at 25 °C. *The Soret region*: A mixture of Zn-MP or Fe-MP (5.0 μM) and the peptide dendrimers (7.0 μM per 2α-helix) was dissolved in 20 mM Tris HCl buffer, pH 7.4, and the samples were equilibrated for 20 min at 25 °C.

UV/Vis measurements: UV/Vis spectra were recorded on a Shimadzu UV-3100 spectrophotometer by using a quartz cell with a 10 mm pathlength. Fe-MP and Zn-MP bindings were measured by titration of the peptide dendrimer in 20 mM Tris HCl buffer, pH 7.4, [Fe-MP] = [Zn-MP] = 5.0 μM. After the addition of the peptide dendrimers, the samples were equilibrated for 20 min at 25 °C. The increase of the Soret absorption maxima at 404 nm (Fe-MP) or 415 nm (Zn-MP) with increased 2α-helix concentration of the peptide dendrimer was fitted to a single-site binding equation.[18]

2-Methoxyphenol oxidation measurements: The 2-methoxyphenol oxidation activity of Fe-MP in the presence or absence of the peptide dendrimers was assayed by measuring the absorbance of the produced tetramer at 470 nm ($\varepsilon = 2.66 \times 10^4\,\text{M}^{-1}\text{cm}^{-1}$).[4a,b] The reaction was initiated by the addition of hydrogen peroxide (0.5 mM) to a mixture of 2-methoxyphenol (10 mM), Fe-MP (5.0 μM), and the peptide dendrimer (7.0 μM per 2α-helix) in 0.1 M Tris HCl buffer, pH 7.4 at 25 °C.

Fluorescence measurements: Fluorescence spectra were recorded on a Hitachi F-2500 fluorescence spectrophotometer with a quartz cell (5 × 5 mm). Methylviologen (MV^{2+}, 0–100 μM) was added to a mixture of Zn-MP (5.0 μM) and the peptide dendrimer (7.0 μM per 2α-helix) in 20 mM Tris HCl buffer, pH 7.4. After each addition of MV^{2+}, the sample was equilibrated for 20 min at 25 °C. Then fluorescence spectra were measured upon excitation at the Q-band ($\lambda_{ex} = 545$ nm, $\lambda_{em} = 560$–700 nm). The decreases of fluorescence at the peak (584 nm) with increasing MV^{2+} concentration were fitted to the Stern–Volmer equation.[19] Fluorescence lifetime was measured by a time-correlated single-photon counting method on a Horiba NAES-550 system. A self-oscillating flash lamp filled with hydrogen was used as a light source. The excitation beam was passed through the Toshiba KL-54 band path filter (545 nm), and the emission beam through the Toshiba R-57 cut-off filter (< 570 nm removed). The lifetimes were obtained by deconvolution with a nonlinear least-squares fitting procedure with a double exponential equation.[10b]

Photoreduction of methylviologen: A mixture of triethanolamine (330 mM), Zn-MP (5.0 μM), the peptide dendrimer (7.0 μM per 2α-helix) and MV^{2+}(50 μM) in 20 mM Tris HCl buffer (pH 7.4) was deaerated by repeated freeze-pump-thaw cycles and then irradiated by a 500 W Xe lamp (Ushio Electric Inc, UI-501C) at 25 °C.[22] Light of a wavelength less than 380 nm was removed by a Toshiba L-38 cut-off filter. The reaction was followed by monitoring the absorbance change of the reduced MV^+ radical at 602 nm ($\varepsilon = 1.37 \times 10^4\,\text{M}^{-1}\text{cm}^{-1}$).[22]

Acknowledgements

We are grateful to Dr. K. Aoi, Nagoya University, for various discussions on dendrimers; Dr. F. Arisaka, Tokyo Institute of Technology, for ultracentrifugation analyses; and Dr. S. Sakamoto, Tokyo Institute of Technology, for various discussions on de novo design.

[1] a) J. R. Darwent, P. Douglas, A. Harriman, G. Porter, M. C. Richoux, *Coord. Chem. Rev.* **1982**, *44*, 83–126; b) I. Okura, *Coord. Chem. Rev.* **1985**, *68*, 53–99; c) M. D. Ward, *Chem. Soc. Rev.* **1997**, *26*, 365–375; d) Y. Z. Hu, H. Takashima, S. Tsukiji, S. Shinkai, T. Nagamune, S. Oishi, I. Hamachi, *Chem. Eur. J.* **2000**, *6*, 1907–1916; e) Y. Z. Hu, S. Tsukiji, S. Shinkai, S. Oishi, I. Hamachi, *J. Am. Chem. Soc.* **2000**, *122*, 241–253; f) P. R. Ashton, R. Ballardini, V. Balzani, A. Credi, K. R. Dress, E. Ishow, C. J. Kleverlaan, O. Kocian, J. A. Preece, N. Spencer, J. F. Stoddart, M. Venturi, S. Wegner, *Chem. Eur. J.* **2000**, *6*, 3558–3574.

[2] a) G. McDermott, S. M. Prince, A. A. Freer, A. M. Hawthornthwaite-Lawless, M. Z. Papiz, R. J. Cogdell, N. W. Isaacs, *Nature* **1995**, *374*, 517–521; b) R. van Grondelle, O. J. G. Somsen in *Resonance Energy Transfer* (Eds.: D. L. Andrews, A. A. Demidov), Wiley, New York, **1999**, pp. 366–398.

[3] a) F. Rabanal, W. F. DeGrado, P. L. Dutton, *J. Am. Chem. Soc.* **1996**, *118*, 473–474; b) H. K. Rau, W. Haehnel, *J. Am. Chem. Soc.* **1998**, *120*, 468–476; c) A. Kashiwada, N. Nishino, Z. Y. Wang, T. Nozawa, M. Kobayashi, M. Nango, *Chem. Lett.* **1999**, 1301–1302.

[4] a) S. Sakamoto, A. Ueno, H. Mihara, *J. Chem. Soc. Perkin Trans. 2* **1999**, 2059–2069; b) S. Sakamoto, A. Ueno, H. Mihara, *J. Chem. Soc. Perkin Trans. 2* **1998**, 2395–2404; c) S. Sakamoto, A. Ueno, H. Mihara, *Chem. Commun.* **1998**, 1073–1074; d) I. Obataya, S. Sakamoto, A. Ueno, H. Mihara, *Protein Pept. Lett.* **1999**, *6*, 141–144.

[5] a) H. L. Anderson, *Chem. Commun.* **1999**, 2323–2330; b) R. K. Lammi, A. Ambroise, T. Balasubramanian, R. W. Wanger, D. F. Bocian, D. Holten, J. S. Lindsey, *J. Am. Chem. Soc.* **2000**, *122*, 7579–7591; c) A. Nakano, T. Yamazaki, Y. Nishimura, I. Yamazaki, A. Osuka, *Chem. Eur. J.* **2000**, *6*, 3254–3271; d) N. Aratani, A. Osuka, Y. H. Kim, D. A. Jeong, D. Kim, *Angew. Chem.* **2000**, *112*, 1517–1521; *Angew. Chem. Int. Ed.* **2000**, *39*, 1458–1462; e) E. B. Fisher, A. M. Shachter, *Inorg. Chem.* **1991**, *30*, 3763–3769; f) O. Mongin, N. Hoyler, A. Gossauer, *Eur. J. Org. Chem.* **2000**, 1193–1197; g) A. Prodi, M. T. Indelli, C. J. Kleverlaan, F. Scandola, E. Alessio, T. Gianferrara, L. Marzilli, *Chem. Eur. J.* **1999**, *5*, 2668–2679.

[6] a) D. A. Tomalia, H. Baker, J. Dewald, M. Hall, G. Kallos, S. Martin, J. Roeck, J. Ryder, P. Smith, *Polymer J.* **1985**, *17*, 117–132; b) D. A. Tomalia, A. M. Naylor, W. A. Goddard III, *Angew. Chem.* **1990**, *102*, 119–157; *Angew. Chem. Int. Ed. Engl.* **1990**, *29*, 138–175.

[7] a) D. K. Smith, F. Diederich, *Chem. Eur. J.* **1998**, *4*, 1353–1361; b) A. Archut, F. Vögtle, *Chem. Soc. Rev.* **1998**, *27*, 233–240; c) M. A. Hearshaw, J. R. Moss, *Chem. Commun.* **1999**, 1–8; d) N. Ardon, D. Astruc, *Bull. Soc. Chim. Fr.* **1995**, *132*, 875–909.

[8] a) D. A. Tomalia, P. R. Dvornic, *Nature* **1994**, *372*, 617–619; b) J. W. J. Knapen, A. W. Van der Made, J. C. De Wilde, P. W. N. M. van Leeuwen, P. Wijkens, D. M. Grove, G. van Koten, *Nature* **1994**, *372*, 659–663; c) L. Balogh, D. A. Tomalia, *J. Am. Chem. Soc.* **1998**, *120*, 7355–7356; d) M. Zhao, R. M. Crooks, *Angew. Chem.* **1999**, *111*, 375–377; *Angew. Chem. Int. Ed.* **1999**, *38*, 364–366; e) B. Bhyrappa, G. Vaijayanthimala, *J. Am. Chem. Soc.* **1999**, *121*, 262–263; f) S. Nlate, J. Ruiz, V. Sartor, R. Navarro, J. C. Blais, D. Astruc, *Chem. Eur. J.* **2000**, *6*, 2544–2553.

[9] a) J. F. G. A. Jansen, E. M. M. Branander-van den Berg, E. W. Meijer, *Science* **1994**, *266*, 1226–1229; b) K. Aoi, K. Itoh, M. Okada, *Macromolecules* **1995**, *28*, 5391–5393; c) F. Zeng, S. Zimmerman, *Chem. Rev.* **1997**, *97*, 1681–1712; d) G. R. Newkome, E. He, C. N. Moorefield, *Chem. Rev.* **1999**, *99*, 1689–1746.

[10] a) A. Adronov, J. M. Frèchet, *Chem. Commun.* **2000**, 1701–1710; b) R. Sadamoto, N. Tomioka, T. Aida, *J. Am. Chem. Soc.* **1996**, *118*, 3978–3979; c) D. L. Jiang, T. Aida, *J. Am. Chem. Soc.* **1998**, *120*, 10895–10901; d) N. Tomioka, D. Takasu, T. Takahashi, T. Aida, *Angew. Chem.* **1998**, *110*, 1611–1614; *Angew. Chem. Int. Ed.* **1998**, *37*, 1531–1534; e) V. Balzani, S. Campagna, G. Denti, A. Juris, S. Serroni, M. Venturi, *Acc. Chem. Res.* **1998**, *31*, 26–34; f) N. Maruo, M. Uchiyama, T. Kato, T. Arai, H. Akisada, N. Nishino, *Chem. Commun.* **1999**, 2057–2058; g) T. Kato, M. Uchiyama, N. Maruo, T. Arai, N. Nishino, *Chem. Lett.* **2000**, 144–145; h) G. M. Stewart, M. A. Fox, *J. Am. Chem. Soc.* **1996**, *118*, 4354–4360; i) A. B. Harim, J. Klafter, *J. Phys. Chem. B* **1998**, *102*, 1662–1664; j) C. Devadoss, P. Bharathi, J. S. Moore, *J. Am. Chem. Soc.* **1996**, *118*, 9635–9644.

[11] M. Sakamoto, A. Ueno, H. Mihara, *Chem. Commun.* **2000**, 1741–1742.

[12] a) C. Rao, J. P. Tam, *J. Am. Chem. Soc.* **1994**, *116*, 6975–6976; b) P. Veprek, J. Jezek, *J. Pept. Sci.* **1999**, *5*, 5–23.

[13] C. L. Bird, A. T. Kuhn, *Chem. Soc. Rev.* **1981**, *10*, 49–82.

[14] E. Atherton, R. C. Sheppard, *Solid Phase Peptide Synthesis: A Practical Approach*, IRL Press, Oxford, UK, **1989**.
[15] J. Meienhofer in *The Peptides*, *Vol. 1* (Eds.: E. Gross, J. Meienhofer), Academic Press, New York, **1979**, pp. 263 – 314.
[16] a) S. Futaki, M. Aoki, M. Fukuda, F. Kondo, M. Niwa, K. Kitagawa, Y. Nakaya, *Tetrahedron Lett.* **1997**, *38*, 7071 – 7074; b) A. K. Wong, M. P. Jacobsen, D. J. Winzor, D. P. Fairlie, *J. Am. Chem. Soc.* **1998**, *120*, 3836 – 3841; c) G. Tuchscherer, M. Mutter, *J. Pept. Sci.* **1995**, *1*, 3 – 10; d) P. E. Dawson, S. B. H. Kent, *J. Am. Chem. Soc.* **1993**, *115*, 7263 – 7266.
[17] J. M. Scholtz, H. Qian, E. J. York, J. M. Stewart, R. L. Baldwin, *Biopolymers* **1991**, *31*, 1463 – 1470.
[18] T. Kuwabara, A. Nakamura, A. Ueno, F. Toda, *J. Phys. Chem.* **1994**, *98*, 6297 – 6303.
[19] D. T. Cramb, S. C. Beck, *J. Photochem. Photobiol. A* **2000**, *134*, 87 – 95.
[20] D. L. Akins, S. Özçelik, H. R. Zhu, C. Guo, *J. Phys. Chem.* **1996**, *100*, 14390 – 14396.
[21] C. G. dos Remedios, P. D. J. Moens in *Resonance Energy Transfer* (Eds: D. L. Andrews, A. A. Demidov), Wiley, New York, **1999**, pp. 1 – 64.
[22] a) T. Watanabe, K. Honda, *J. Phys. Chem.* **1982**, *86*, 2617 – 2619; b) S. Aono, I. Okura, *J. Phys. Chem.* **1985**, *89*, 1593 – 1598; c) I. Okura, Y. Kinumi, *Bull. Chem. Soc. Jpn.* **1990**, *63*, 2922 – 2927; d) G. McLendon, D. S. Miller, *J. Chem. Soc. Chem. Commun.* **1980**, 533 – 534.
[23] M. Sakamoto, T. Kamachi, I. Okura, A. Ueno, H. Mihara, *Biopolymers* **2001**, in press.
[24] J. W. Buchler in *The Porphyrins*, *Vol. 1* (Ed.: D. Dolphin), Academic Press, New York, **1978**, pp. 389 – 483.

Received: November 17, 2000 [F2876]

  0947-6539/01/0711-2458 $ 17.50+.50/0